

## The Damage Mechanics of Creep Thickness Effects of the Single Crystal Superalloys.

Brice Cassenti<sup>(1a)</sup> and Alexander Staroselsky<sup>(2b)</sup>

<sup>1</sup>Rensselaer Polytechnic Institute, 275 Windsor St, Hartford, CT 06120 USA

<sup>2</sup>Pratt & Whitney, 400 Main Street, East Hartford, CT 06108 USA

<sup>a</sup>[casseb@rpi.edu](mailto:casseb@rpi.edu); <sup>b</sup>[alexander.staroselsky@pw.utc.com](mailto:alexander.staroselsky@pw.utc.com)

**Keywords:** Damage, creep, size effects, superalloy

**Abstract.** The micromechanics of the high temperature creep and damage accumulation in single crystal nickel base superalloys is important for the design of turbine airfoils in advanced gas turbines. Advanced turbine blades are typically thin-walled cooled structures made of single crystal nickel base superalloys. Testing has shown that the creep response is larger in thin wall structures than in test specimens typically used to characterize the material. It also has been experimentally observed that creep rupture lives obtained at moderate to high temperatures decreased sharply (~60%) with a reduction in specimen thickness in approximately eight times. We have developed a dislocation-based creep damage model explaining this effect. The model considers the interaction of dislocations with the surface and the effect of nucleated intrusions or/and extrusions on creep strain rate. Based on micromechanical analysis we introduced the appropriate damage mechanics parameter and deduced its evolution kinetics. We were able to accurately predict thin wall creep debit effect during tertiary creep stage and estimated creep time to rupture for different specimens thicknesses. Model predictions were verified against experimental data.

### Introduction

Advanced aircraft engine components can be subjected to a large number of thermo-mechanical loading cycles and to long dwell times at high temperatures in a hostile environment. The focus here is on a specific aspect of this complex multi-scale problem: the effect of section thickness on the creep life of turbine blades. As turbine design has advanced, the cooling passages in single crystal super-alloy turbine blades have become increasingly complex, leading to blades with significantly reduced thickness. Also, overall requirements for weight reduction drive designs toward thinning of the effective airfoil walls. There is a variety of experimental evidence indicating that the reduced section thickness leads to creep rates greater than what would be predicted based on the creep response of thicker sections. This is referred to as the thickness debit effect. Curves of creep strain versus time are shown in Fig. 1, taken from [1], that illustrates the thickness debit effect.

The values of sheet thickness in Fig. 1 vary by nearly an order of magnitude and the thinner specimens are the more rapid accumulation of creep strain is evident. Several mechanisms have been proposed in the literature to account for the thickness debit effect. Baldan [2] argued that the

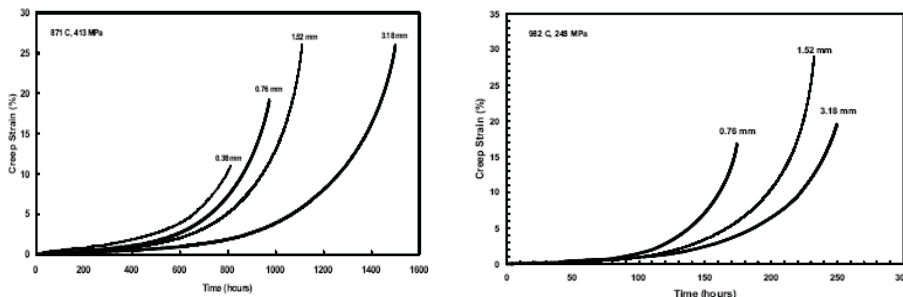


Figure 1: Plot of experimental data from [1] showing the effect of specimen thickness on the creep strain versus time response for single crystal nickel based super alloy specimens: (a) 871°C/413 MPa and (b) 982°C/248 MPa.

creep response is controlled by the crack size to section size ratio. He presumed that the damage mechanism responsible for the thickness debit effect occurred throughout the section. Seetharaman and Cetel [1] considered several possible explanations including cavity nucleation, growth and coalescence.

Obviously, both experiments and practical experience demonstrate that the nature and extent of the thin wall debit are still not well understood and additional work needs to be done to explain, and reliably predict, the amount of additional creep and damage associated with thin sections. Experimental data [1-4] known to the authors clearly demonstrate that the thin wall effect takes place if the section thickness becomes less than 20-40 mils (0.5-1 mm). Since the size of the  $\gamma'$  precipitates is less than 1  $\mu\text{m}$ , which is about three orders of magnitude smaller, the two-phase nature of intermetallic cannot be the direct cause of the observed effect. The typical size of the micro pore is about 10 - 20  $\mu\text{m}$  [5], which is also at least two orders of magnitude smaller than characteristic thickness. During the analyses we will assume that neither  $\gamma'$  particles nor initial porosity plays a significant role in the thin wall debit effect. Nevertheless, microstructure is crucial in modeling damage accumulation in order to predict creep curves. Test results obtained in [3] showed that the thin section thickness debit of uncoated specimens was considerable while the rupture lives of coated specimens were essentially independent of section thickness. These clearly illustrate that the thin wall debit depends on surface effects and specifically on degradation mechanisms taking place primarily in the specimen surface and subsurface zones. Extensive testing of both coated and uncoated PWA 1480 specimens when the section thickness was reduced to 0.25 mm (10 mils) [4] demonstrated a debit of 30-40% in creep rupture strength for all conditions.

It is worthwhile to note that the discussed effect of creep strength reduction with a decrease of the specimen thickness is completely opposite to the known scale effects in fracture mechanics [6] and plasticity [7]. In both these phenomena the strength of the specimen increases with a decrease in the specimen size. Despite different scale effects explanations based on statistics of defect distributions in fracture mechanics, and on specific hardening due to strain gradients in plasticity, will predict a strength increase with a size decrease within reasonably broad limits. In this paper we consider the opposite effect specific for creep deformation. Hence, neither of these approaches can be employed for thin wall debit modeling.

## Viscoplastic model.

It is generally accepted that creep deformation starts by the generation and glide of octahedral dislocations of the type  $\{111\}\langle 110\rangle$  in  $\gamma$  channels. These dislocations overcome the  $\gamma'$  particle by combination of slip and climb. It is also possible that the dislocations or their reaction products cut through the  $\gamma'$  particle if the applied stress is high enough to overcome the threshold. At high stresses and/or high temperatures the secondary cube slip systems  $\{100\}\langle 110\rangle$  can also be activated. There are 12 octahedral slip systems and 6 cube slip systems in Ni-based superalloys. In bulk solids the inelastic flow is initiated by dislocations multiplication typically from Frank–Read sources. The dislocations glide, interacting with other dislocations in the solid and are immobilized, generating pinned dislocations. If the samples are thin, dislocation loops annihilate by interaction with the free surface creating intrusions or extrusions.

According to the Orowan assumption, creep strain rate is proportional to the density of the mobile dislocations  $\rho_m$ , magnitude of the Burgers vector,  $b$ , and their average velocity. If we denote an arbitrary reference dislocation density throughout  $\rho_0$ , the dimensionless parameter  $\frac{\rho_m}{\rho_0}$  serves as a measure of the mobile dislocation density, and can be used to predict tertiary creep. We have used a standard viscoplastic power law creep with a back stress [8] to represent the response of the material. The constitutive law for the inelastic strain,  $\gamma_i^p$  along slip plane  $i$  will be written as follows:

$$\dot{\gamma}_i^p = \dot{\gamma}_0 \left( \frac{\rho_m}{\rho_0} \right) \left( \frac{\tau_i - \omega_i}{s_i^*} \right)^n \operatorname{sgn} \left( \frac{\tau_i - \omega_i}{s_i^*} \right), \quad (1)$$

where  $\dot{\gamma}_0$  is a time constant,  $\tau_i$  is the slip plane resolved shear stress,  $s_i^*$  is the isotropic yield stress,  $\omega_i$  is the slip plane back stress, and  $(\dot{\phantom{x}})$  is the rate of change with respect to time. The isotropic yield stress  $s_i^*$  is assumed to be a constant throughout this discussion but is actually a variable with its own evolution equation. The total inelastic strain rate is considered in this work as a direct sum of the creep and the instantaneous plastic incremental strain. Plastic shear rate is taken in rate dependent form using a high power exponent leading to very low strain rate sensitivity. Effect of voids on the creep rate can be calculated throughout effective increase of the resolved shears. Dislocation generation and motion represent a non-recoverable state for the material. These states can be related to the energy for the system through equilibrium statistical mechanics. We postulate that dislocation generation rate is proportional to the entropy production. Using concepts from chemical kinetics we have chosen to represent the evolution as two body interactions. We assume that dislocation immobilization takes place when two corresponding dislocation loops interact with each other. Taking into account that  $\{\dot{\gamma}^c\}^\alpha$  is already a linear function of the mobile dislocation density to represent two body interactions we obtain relations for mobile and pinned dislocations along each slip system:

$$\begin{aligned} \dot{\rho}_m^\alpha &= M \left( \frac{\tau^\alpha - \omega^\alpha}{s^\alpha} \right) \dot{\gamma}_m^\alpha \left( \frac{\varepsilon^2 \rho_m^{ss} + \rho_p^{ss} - \rho_p^\alpha - \varepsilon^2 \rho_m^\alpha}{\rho_0} - C v^{2/3} \right) (1 - v) \\ \dot{\rho}_p &= \Pi \left( \frac{\tau^\alpha - \omega^\alpha}{s^\alpha} \right) \dot{\gamma}_m^\alpha \left( \frac{\rho_p^{ss} - \rho_p^\alpha}{\rho_0} \right) (1 - v) \end{aligned} \quad (2)$$

where M and  $\Pi$  represents specific time constants, different for octahedral and cube slip systems,  $\rho_m^{ss}$ , is the saturated mobile dislocation density,  $\rho_p^{ss}$ , is the saturated pinned dislocation density, and  $\varepsilon^2$  is a positive constant,  $v$ - is the pores volume fraction. Equations (2) include the annihilation of mobile dislocations and also include their conversion to pinned dislocations. The pinned dislocations grow at a rate that is proportional to the mobile dislocation density because of the presence of the plastic strain rate term.

### Thin Wall Damage

We apply the mesoscale model outlined in the previous section to the explanation of the creep acceleration effect due to the reduced section thickness. Here, we formulate the physical phenomena causing an increase in the applied effective stress and with any decrease of the cross section and estimate the characteristics of the damaged surface layer.

We assume that: 1) dislocation loops are formed usually from Frank-Read type sources, and 2) the distance a dislocation loop moves is limited to the width of the sample. The loop will interact with the free surfaces as shown in Fig. 4 and result in truncated single arms of dislocations forming steps. Each step has a height at least equal to the lattice parameter.

The average total height of observed slip steps varies from several hundreds to several thousands of lattice parameters [9]. In thin samples, where the thicknesses are of the same order of magnitude as the radius of the dislocation loops, most of the loops end up forming the surface slip step. Accordingly, the model assumes a random distribution of dislocation loops with some of them ending at the surface. For a given dislocation, the length and the sign of the surface step (i.e. intrusion or extrusion) depends on Schmidt factors for the slip systems and can be considered as a random variable with a binomial distribution for the direction of the slip. In other words, first we consider slip band propagation and surface interceptions as a random walk process and then estimate the total height of surface slip steps. These steps will decrease the effective area over which shear stresses will act.

Recall that the thin-walled debit is based on the slip induced surface roughness or in other words on the intersection of dislocation loops with the surface. Consider a flat dislocation loop of radius  $R$  with the normal to the plane of the loop at an angle  $\theta$  with respect to the length of a uniaxial stress test specimen. It can be shown that the average density of dislocation loops intercepting the surface,  $N_I$ , for a specimen of thickness  $H$  is

$$N_I = 4\rho_m \frac{\langle R \rangle}{H} \cos\theta \quad (3)$$

here  $\langle R \rangle$  is the average dislocation loop radius. Each surface step shifts the specimen surface in a direction depending on the Burger's vector orientation. For many dislocations intercepting the surface, the average number moving the surface right,  $\mu$  can be found from the binomial

distribution as the half of total interceptions:  $\mu = \frac{N_I}{2}$  while the standard deviation,  $\sigma$ , satisfies  $\sigma^2 = \frac{N_I WL}{4}$  where  $W$  and  $L$  are the width and height (length) of a surface. Then for many interceptions, we could assume the probability distribution in the number of intercepts is normal. If we substitute the mean value and standard deviation calculated into a Gaussian distribution then we can obtain the average absolute distance,  $S$ , each surface moved from the mean (induced surface roughness):

$$S = \frac{b}{\sqrt{2\pi}} \sqrt{N_I WL} \quad (4)$$

where each dislocation has Burger's vector length  $b$ .

It is important to emphasize that we describe here a mechanism of initiation of a damaged surface layer specific for the material structure. The proposed mechanism might be complimented by other surface effects such as, for example, oxidation or sub-surface microstructure degradation and we do not evaluate them in this methodological work. Our basic assumption is that this damaged surface layer is material structure specific and does not depend directly on loading or geometry. Following surface damage initiation, the overstressed boundary layer is created, which in turn initiates the creation of active voids and microcracks and their subsequent growth.

We can find the increase in the cross-section stress by applying the fracture mechanics model for surface cracks of length  $S$  and average the local stress over the cross-section. Combining the applied stress,  $\sigma_0$ , with the averaged local effects we obtained the effective stress  $\sigma_L$  according to:

$$\sigma_L = \frac{\sigma_0}{1 - 2S/H} \left( 1 + 2.24 \sqrt{\frac{S/H}{1 - 2S/H}} \right) \quad (5)$$

It can be seen that the effective stress depends on material parameter  $S$  and specimen thickness  $H$  and increases with the decrease of the specimen thickness. However, for relatively thick specimens, the effect of the damage layer is insignificant and does not cause a change in the creep strain rate prediction. Finally, note that the definition of how thick or thin the part section is related to the material specific surface damaged layer or on the scale parameter  $S/H$ . Of course the stress in equation (5) must also be used in the strain rates calculation.

Local overstress due to surface roughness causes non-homogeneous void nucleation and growth. Local effect of voids on the creep rate can be calculated throughout effective increase of the resolved shear:  $\left( \frac{\tau^\alpha}{(1-\nu)} - \omega^\alpha \right) / s_*^\alpha$ , which in turn increases local stress level and increases the creep rate.

As has been shown in [10] the porosity development process for our case is mostly controlled by voids nucleation. Void nucleation is taken to be strain controlled with a normal distribution [11] with

$$\dot{\nu}_{nuc} = \frac{f_N}{\sqrt{2} s_N} \exp \left( -\frac{1}{2} \left( \frac{\epsilon - \epsilon_N}{s_N} \right)^2 \right) \quad (6)$$

where  $f_N$  is value of the volume fraction of voids available for nucleation,  $\epsilon_N$  is the mean void nucleation strain and  $s_N$  is the corresponding standard deviation.

A representative region analyzed is shown in Fig. 2. The possibility of damage nucleation in the form of voids is shown here with contours of  $v_{nuc}$ . The material where damage due to void nucleation and growth is possible is confined to a surface layer. Interior to this boundary layer is the bulk material here no voids are allowed to develop.

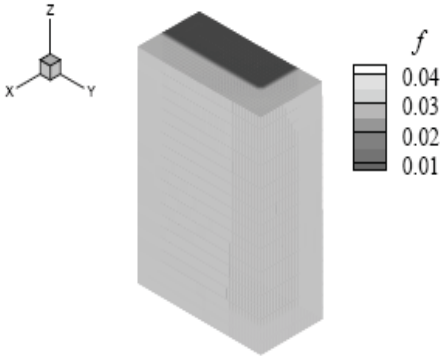


Figure 2. Contours of void volume fraction after deformation of 20% for  $s_{void} = 0.2H$ , where H is the specimen thickness.

13 percent for different flat specimen thicknesses. The applied stress in this calculation has been chosen  $\tau/s_0 = 0.56$ .

The calculated time decreases with a decrease in the specimen thickness H. Let us define the ratio of the calculated time to reach 13% strain to the corresponding time evaluated for the specimen of the thickness of 0.31 cm (125 mils) as the relative life. The relative life is shorter by 28 percent for 0.0375 cm (15 mils) and there is an evident decrease in the rupture life at a thickness below 0.15 cm

We compare the model prediction against experimentally measured creep curve for PWA 1484 in <001> orientation under tension with the nominal stress of 248 MPa (36 ksi) at the temperature of 982 C (1800 F). For the low stress case considered (applied stress is 50% of the yield) the thin wall damage parameter is relatively small, but there is still a significant thin wall debit observed. Although  $S/2H$  is small, the change in the effective applied stress (see eq. 5) might reach 10% and ultimately the creep strain rate becomes significant.

Fig. 3 shows the creep time to reach a strain of

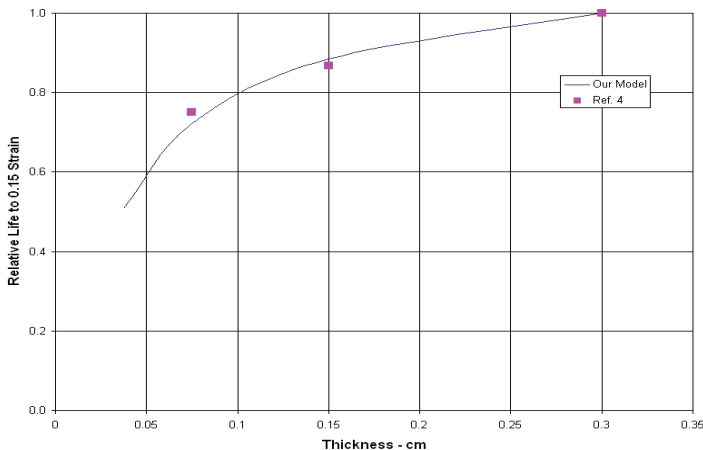


Figure 3. Relative Rupture Life Decrease Example in Thin Wall Structures

(60 mils). The agreement with the test data in reference [1] is exceptional where the relative rupture life was found to decrease to 72 percent at a thickness of 0.075 cm (30 mils).

## Conclusions

A reduced section thickness leads to creep deformation greater than the observed creep response of thicker sections. The discussed effect is completely opposite to the known scale effects in fracture mechanics and plasticity where the structure strength increases with the decrease of the samples. Accounting for the debit in creep life is essential in the design of thin wall single-crystal structures deformation.

A dislocation based material model has been presented for the creep analysis of single crystal superalloys. We show that an analysis of the statistical variation in the dislocation interception with the part free surface allows the introduction of scale parameter rationalizing much of the thin section creep debit effect. The performed creep calculations clearly demonstrate that the effects of the thickness debit can be explained by incorporation of the damage effects confined to the surface layer of the material. We can conclude that meso-scopic surface effects are important and have a significant effect on the macroscopic response of thin wall structures. These effects can be the motion of dislocations induced surface roughness, the preferential generation of voids or micro-cracks near the surface, or even a direct result of surface oxidation. Our model of dislocation loops intersecting the surface shows that the important effect is the effective increase in stress due to surface defects.

Comparison of the model predictions against known test results obtained on single crystals superalloys has shown good agreement with data. Experimental evidence [3] that thin wall debit effect of uncoated specimens was considerable while the rupture lives of coated specimens were essentially independent of section thickness strongly supports the model assumptions.

## References

- [1] V. Seetharaman and Cetel, A. Thickness Debit in Creep Properties of PWA 1484, Superalloys 2004, Edited by K.A. Green, T.M. Pollock, H. Harada, pp. 207-213, 2004
- [4] A. Baldan. On the thin-section size dependent creep strength of a single crystal nickel-base superalloy. *Journal of Materials Science*, 30:6288–6298, 1995.
- [3] M. Doner and J.A. Heckler: “Effects of Section Thickness and Orientation on Creep-Rupture properties of Two Advanced Single Crystal Alloys”, in *SAE Technical Paper # 851785*, Society of Automotive Eng.
- [4] F. Soechting “Thin Wall Debit” Internal Memo, P & W, East Hartford, CT, 1982.
- [5] A. Epishin and T. Link, Mechanisms of High Temperature Creep of Nickel-Base Superalloys Under Low Applied Stress, Superalloys 2004, Edited by K.A. Green, T.M. Pollock, H. Harada, pp. 137-143, 2004,
- [6] A. M. Freudenthal, Statistical approach to brittle fracture. In *Fracture*, Vol. II, Ed. H. Liebowitz, pp 591-621, Academic Press, NY 1968
- [7] Fleck, N.A., Hutchinson, J.W., “A Phenomenological Theory for Strain Gradient Effects in Plasticity” *J. Mech. Phys. Solids* 41 1825-1857, 1993.
- [8] Nissley, D., Meyer, T., and Walker, K. Life Predictions and Constitutive Models for Engine Hot Section Anisotropic Materials, Pratt & Whitney, Report NAS3-23939, 1991 [9] S. Kocanda, Fatigue Failure of Metals, Sijthoff & Noordhoff Int. Publishers, The Netherlands, 1978, 368 p.
- [10] J. Gullickson, A. Needleman, A. Staroselsky, B. Cassenti, Boundary Damage Effects on the Evolution of Creep Strain. Submitted for publication to *Modelling and Simulation in Materials Science and Engineering*
- [11] C. C. Chu and A. Needleman, Void nucleation effects in biaxially stretched sheets. *Journal of Engineering Materials and Technology*, 102:249–256, 1980